Check for updates

# Elucidating the deactivation mechanism of beta zeolite catalyzed linear alkylbenzene production with oxygenated organic compound contaminated feedstocks†

Shiyong Xing, [ID] [a] Xiaofei Liu,[b] Yan Cui,[c] Yuehua Zhao,[b] Ziheng Chen,[b] Sigui Xiang*[a] and Minghan Han*[b]

Zeolite catalyzed alkylation of benzene with long-chain α-olefins is a promising method for the detergent industry. Considering the long-chain α-olefins from Fischer–Tropsch synthesis always contain some oxygenated organic compounds, the effect of which on the alkylation of benzene with 1-dodecene was comprehensively investigated over beta zeolite herein. n-heptanol, n-heptaldehyde and n-heptanoic acid were selected as the model oxygenated organic compounds, and it was revealed that an obvious decrease of lifetime occurred when only trace amount of oxygenated organic compounds were added into the feedstocks. The deactivated catalyst was difficult to regenerate by extraction with hot benzene or coke-burning. A series of characterization tests complementary with DFT calculations revealed that the deactivation was mainly caused by the firm adsorption of oxygenated organic compounds on the acid sites. Further, comparison with the open-framework MWW zeolite revealed a similar effect of oxygenated organic compounds and deactivation mechanism for both beta and MWW, but beta is less sensitive to the oxygenated organic compounds. The main reason lies in the three-dimensional framework of beta, wherein the much higher adsorption energy of 1-dodecene makes it difficult to be replaced by oxygenated organic compounds. Additionally, beta could be regenerated more easily by extraction with hot benzene compared with MWW. But coke-burning caused a sharp decrease of its lifetime, which is mainly due to the decreased acid sites after calcination.

## 1. Introduction

Detergent has been essential to human life for over a thousand years.[1] Linear alkylbenzene (LAB) acts as an important precursor for the production of linear alkylbenzene sulfonic acids (LASs), which are usually manufactured by the alkylation of benzene with long-chain α-olefins (typically, C10–C14). In terms of the excellent biodegradable, high solubility, strong detergent ability and low cost, LASs accounts for the largest part of the detergent market.[2,3] In fact, the development of detergent technology is driven by the so-called green chemistry principle.[1] Conventionally, LAB is synthesized homogeneously in the presence of HF or AlCl₃. However, these two processes suffer

from severe corrosion, low selectivity, separation problems, waste disposal problems, and are environmental hazards.[1,4,5] Therefore, it is highly desirable to develop more eco-friendly and efficient catalytic processes.

In the past decades, a variety of solid acidic catalysts have been investigated for the alkylation of benzene with long-chain α-olefins, including clay,[6,7] zeolite,[8–10] fluorided silica-alumina,[11,12] heteropoly acids (HPAs),[13] metal oxides and sulfides,[2,7,14] etc. A milestone of this developing process was achieved by UOP in 1995.[4] The first solid acidic Detal™ process developed by UOP was based on a fixed bed of a noncorrosive silica-alumina catalyst. However, the cycle length of this process was too short to be industrialized widely. Among the solid acidic catalysts mentioned above, zeolites are the most attractive for researchers, mainly due to their tunable acidic properties, various frameworks, excellent thermal stability and fascinating shape-selectivity. As one of the predecessors, Venuto et al. found that highly acidic faujasites are more active than silica-alumina catalyst.[15] After that, the catalytic potential of numerous zeolites for the LAB production has been demonstrated in searching for eco-friendly LAB process as an alternative of liquid acid catalyst.[1,16]

[a]Beijing Special Engineering Design and Research Institute, Beijing 100028, P. R. China. E-mail: 13717798109@139.com

[b]Beijing Key Laboratory of Green Chemical Reaction Engineering and Technology, Department of Chemical Engineering, Tsinghua University, Beijing 100084, P. R. China. E-mail: hanmh@mail.tsinghua.edu.cn

[c]Petrochemical Research Institute, PetroChina Company Limited, Beijing 100195, China

For example, Cao *et al.* compared three zeolites with different frameworks for the alkylation of benzene with 1-dodecene, and found that both ZSM-5 and ZSM-11 were inactive mainly due to their restricted channels. While beta and FAU zeolites with 12 member-ring framework were proved to be more active.[17] Regarding the large pore size zeolites, Waqas *et al.* investigated the alkylation of benzene with 1-dodecene over three 12 member-ring zeolites, and found that FAU is more active and stable than beta and MOR. However, the subsequent desilication enable beta and MOR more hierarchical porous structures and low Si/Al, by which enhanced catalytic performance was obtained thereof.[18] Similarly, for the low stability of MOR with one-dimensional framework, desilication was proved to be more effective to improve its lifetime compared with other approaches such as dealumination or metal/zeolite.[19] In our previous research, we found that the stability of microporous beta zeolite can be effectively enhanced by decreasing crystal size or constructing micro–meso composites when used for the LAB synthesis.[20,21] In fact, the selectivity is also very sensitive to the framework. For example, although both FAU and EMT all own three-dimensional channels, subtle differences between them still results in dramatic increase of 2-LAB selectivity from 28% for FAU to 42% for EMT.[17] Wang *et al.* reviewed the most investigated zeolites for the LAB production in the past decades, and found that MOR and MTW with one-dimensional framework are more selective for 2-LAB.[4]

As discussed above, the catalytic performance of the zeolite catalyzed alkylation of benzene with long-chain $\alpha$-olefines is highly correlated with the zeolite frameworks. In fact, this structure-reactivity is a hot debated topic in the catalytic field for a long time, and can also be reflected in a variety of reaction systems, including alkylation of benzene with ethene/propene,[22–25] alkane cracking,[26,27] isomerization of alkane,[28] *etc.* And deep understanding the structure-reactivity is really significant for the catalyst design. Therefore, for the present work, finding or designing catalysts with suitable framework is decisive to the catalytic performance for the LAB production. And at the same time, the cost should also be considered for the industrial utilization.

Generally, ethene and propene are the important indicators reflecting the developing level of petrochemical industry and economic development of every country. However, the development of petroleum to olefins is limited by the shortage of oil in China. It is of great importance to find alternative route for olefin production.[29] From the perspective of resource reserves and strategic safety, the coal-to-olefin route is an important direction for the sustainable development of chemical industry.[30] Fortunately, this technology has been successfully industrialized in China.[31] Regarding the present work, $\alpha$-olefins from petrochemical can also be replaced with coals, which acts as a typical example of coal chemicals. However, the products from coal-to-olefin always contain some oxygenated organic compounds. In our previous investigation, these oxygenated organic compounds were proved to be detrimental to MWW zeolite with open-framework when catalyzing the LAB synthesis, and the oxygenated organic compounds should be restricted to be at least lower than 28 ppm.[32] To the best of our knowledge,

the effect of oxygenated organic compounds on the zeolite with different frameworks was rarely studied by others and whether the structure of zeolite can influence the effect of oxygenated organic compounds is also unknown but worth investigating.

Therefore, beta zeolite with 12 member-ring and three-dimensional framework was selected herein to elucidate the effect of oxygenated organic compounds on the alkylation of benzene with 1-dodecene. Three representative organics, *e.g.*, *n*-heptanol, *n*-heptaldehyde and *n*-heptanoic acid were selected as the model oxygenated organic compounds, mainly due to their higher content in the kerosene distillate from Fischer–Tropsch synthesis. The effect of oxygenated organic compounds amount and type were systemically studied. It's revealed that trace amount of oxygenated organic compounds could cause obvious decrease of the lifetime, and the deactivation was mainly caused by the firm occupation of oxygenated organic compounds on the acid sites of zeolite. The regeneration processes of both extraction with hot benzene and coke-burning were also considered. Further comparison with MWW zeolite was discussed.

## 2. Methods

### 2.1. Experimental

**2.1.1. Materials.** The feedstocks, benzene (>99.5%) and 1-dodecene (95%) were purchased from the Beijing Tong Guang Fine Chemicals Company and Aladdin Chemical Reagent Company, respectively. Both *n*-heptaldehyde (97%) and *n*-heptanoic acid (98%) were all supplied by Meryer (Shanghai) Chemical Technology Co., Ltd. and *n*-heptanol (98.5%) was obtained from the Titan Technology Corporation. All reagents were stored in fume hoods and commercially received without further purification. Beta zeolite was synthesized according to the method describe in ref. 33.

**2.1.2. Catalytic evaluation.** The alkylation of benzene with 1-dodecene was performed in a continuous-flow fixed bed micro-reactor (see Fig. S1†) at 4.2 MPa, consisting of a stainless tube reactor with a length of 50 cm and a diameter of 1 cm. A typical experiment was performed using 1 g catalyst mixed with 10 g quartz sand. Before reaction, the catalyst was activated under 100 ml min$^{-1}$ $N_2$ flow for 3 h at 300 °C. After cooled to 100 °C, benzene was firstly pumped into the reactor to reach 4.2 MPa and then the mixture of benzene/1-dodecene with molar ratio of 15/1 (benzene/1-dodecene) was switched into the reactor. Different amounts of oxygenated organic compounds were added into the reaction mixtures where needed. It should be noted that all steps of the preparation of feedstocks was conducted in fume hoods. The effluent mixture was analyzed offline with a gas chromatograph (Shimadzu GC-14B) equipped with a flame ionization detector (FID). The catalyst was assumed to be deactivated as the conversion of 1-dodecene decreased below 95%, and then the lifetime was calculated thereof. It should be noted that B-fresh, B-heptanol, B-heptaldehyde, B-heptanoic acid and B-coke appearing in the following text represent the fresh beta zeolite, and the deactivated beta caused by *n*-heptanol, *n*-heptaldehyde and *n*-heptanoic acid and coke, respectively.

**2.1.3. Catalyst characterization.** The crystalline structure of the samples was determined by Powder X-ray diffraction (XRD)

using a Bruker D8 Advance powder X-ray diffractometer with Cu Kα radiation. The scanning range of 2θ was 2–50° at 2° min⁻¹. A physisorption analyzer (Quantachrome Autosorb iQ) was used to measure the surface areas and pore structure of different samples at 77 K. For the morphology study, different samples were investigated by scanning electron microscopy (SEM) characterization conducted with a JSM7401 instrument. Transmission electron microscopy (TEM) images were recorded on a JEM2010 at 200 kV. Thermo-gravimetric analysis (TGA) and differential thermal analysis (DTA) experiments were performed on a TGA/DSC1/1600LF apparatus. The experiments were carried out in a temperature range of 25–800 °C under flowing air (100 ml min⁻¹), and with a heating rate of 10 °C min⁻¹. IR spectra of KBr-diluted wafers of the zeolite samples were recorded by a Ncxus670 spectrometer equipped with a MCT detector and a KBr beam splitter.

### 2.2. Computational details

All periodic DFT calculations were performed using the Vienna *Ab initio* Simulation Package (VASP 5.3.5)[34,35] with the Grimme's D3 corrections[36] to describe the vdW interactions. The projector augmented wave (PAW) method[37,38] was used to describe the electron–ion interaction with the plane wave basis set kinetic energy cutoff of 400 eV. The Brillouin zone was sampled at the $\Gamma$ point only by using the Monkhorst–Pack technique.[39] A force threshold of 0.02 eV Å⁻¹ was used for the geometry optimization of all intermediates.

The BEA cell was constructed according to the Structure Commission of the International Zeolite Association.[40] Firstly, the all-silicon form of BEA cell was constructed in 1 × 1 × 1. The lattice constants were then optimized (12.66, 12.66, and 26.58 Å) by using an energy cutoff of 600 eV and a force threshold of 0.01 eV Å⁻¹. Considering a larger length of 1-dodecene, the 1 × 1 × 1 BEA cell will be extended when calculating the adsorption energy of 1-dodecene. For H-BEA, the substitution of Si atom with Al atom at T9 is energetically most favorable as suggested by previous works.[41–44] The information of the optimized geometries of H-BEA is shown in Fig. 1.

The adsorption energy of guest species in zeolites was calculated as follows:



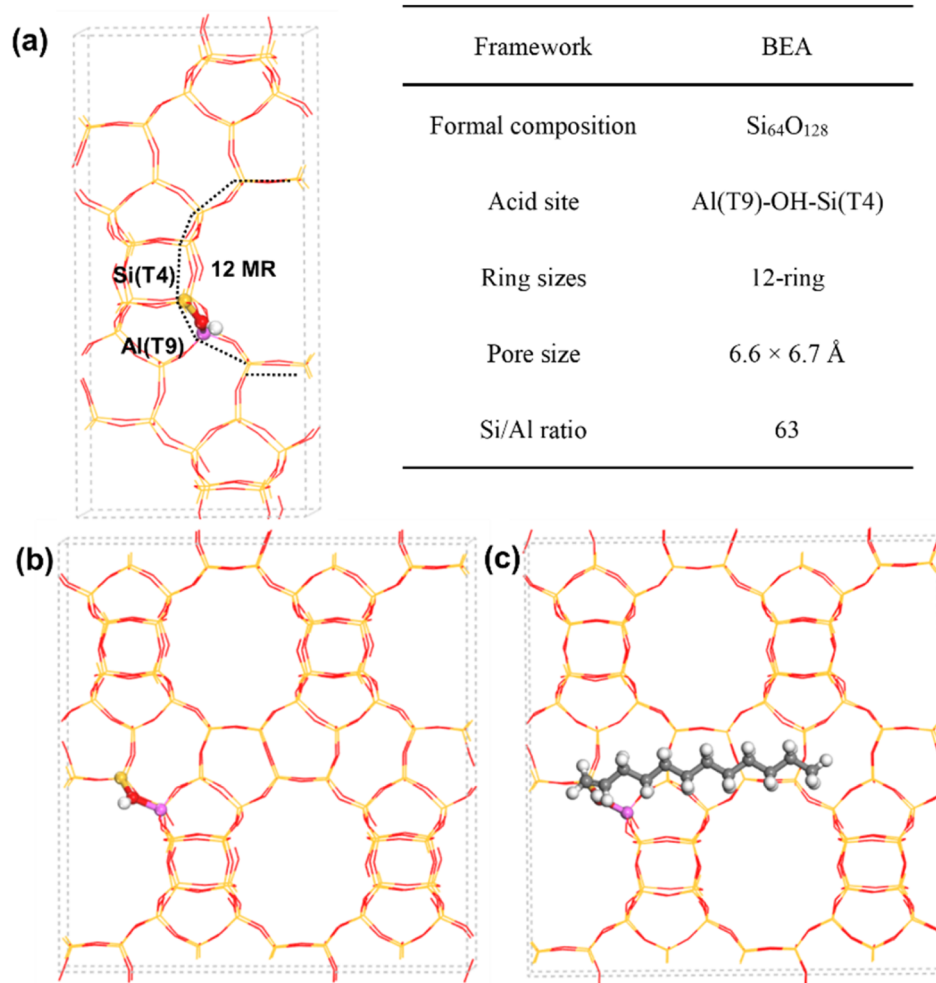| Framework | BEA |
|---|---|
| Formal composition | $Si_{64}O_{128}$ |
| Acid site | Al(T9)-OH-Si(T4) |
| Ring sizes | 12-ring |
| Pore size | 6.6 × 6.7 Å |
| Si/Al ratio | 63 |

Fig. 1 Geometry structures of H-BEA. (a) Single BEA cell, (b) extended BEA cell and (c) 1-dodecene adsorbed on the extended BEA cell. Yellow: silicon; red: oxygen; purple: aluminum; white: hydrogen; gray: carbon. T represents the tetrahedral Si or Al atom. The color scheme is used throughout the paper.

$$\Delta E_{ads} = E_{adsorbate/H\text{-}zeolite} - E_{adsorbate} - E_{H\text{-}zeolite} \tag{1}$$

The fundamental terms $E_{adsorbate/H\text{-}zeolite}$ and $E_{H\text{-}zeolite}$ are the energies of the zeolite cell with and without adsorbate respectively, and $E_{adsorbate}$ is the energy of the isolated adsorbate.

## 3. Results and discussion

### 3.1. Effect of oxygenated organic compounds on the catalytic performance

Herein, beta was selected as the solid acid catalyst to investigate the effect of oxygenated organic compounds on the alkylation of benzene with 1-dodecene. As shown in Fig. 2a, it's not easy to distinguish the precise crystal size and morphology of beta zeolite by SEM, which is mainly due to its nano-sized crystals. Fortunately, the crystals can be more clearly observed by TEM (see Fig. 2b), wherein the ordered micropores imply its high crystalline. The fringes of the crystals is not uniform, which is mainly due to its small crystals.[21] The XRD patterns of the as-synthesized beta are shown in Fig. 2c, wherein the distinct diffraction peaks at 7.5° and 22.5° are well consistent with the previous publications, implying its high purity.[21,33] As can be seen from the $N_2$ sorption isotherms shown in Fig. 2d, beta exhibits the typical I-type isotherms, indicative of its high crystalline of micropores. The distinct adsorption of $N_2$ at the low-pressure range denotes its large proportion of micropores. Additionally, a hysteresis loop exists in $0.5 < P/P_0 < 1.0$, indicating the existence of mesopores and macropores. In fact, these mesopores and macropores should be mainly formed in between the space of the aggregated crystals.

Firstly, we select $n$-heptanol as the main model oxygenated organic compounds to illustrate their effects on the zeolite catalyzed LAB synthesis, and the specific results are shown in Fig. 3a and b. As can be seen, the lifetime decreases obvious only after trace amount of $n$-heptanol added into the feedstocks. As the amount of $n$-heptanol increases, the lifetime decreases gradually at the same time. Therefore, it can be inferred that there may exist competitive adsorption between oxygenated organic compounds and reactants (benzene/1-dodecene) on the acid sites. As the oxygenated organic compounds amount in the feedstocks exceeds 100 ppm, more than 32% of lifetime was lost. Considering the complex composition of oxygenated organic compounds from Fischer–Tropsch synthesis, the effect of other oxygenated organic compounds (viz., $n$-heptaldehyde and $n$-heptanoic acid) were also considered. As can be seen from Fig. 3c and d, both of them were all proved to be deleterious to the catalytic performance, and it seems that beta is more sensitive to these two compounds. In fact, $H_2O$ is also an impurity in the feedstocks, the effect of it on the reaction was also considered. As can be seen from Fig. 3c and d, $H_2O$ exhibits a similar effect with $n$-heptanol. Fortunately, it's easier to separate $H_2O$ from the feedstocks compared with other oxygenated organic compounds, mainly for the distinct boiling point difference between $H_2O$ and other molecules. Considering the higher content and separation cost of the organic oxygenated organic compounds (such as, $n$-heptanol, $n$-
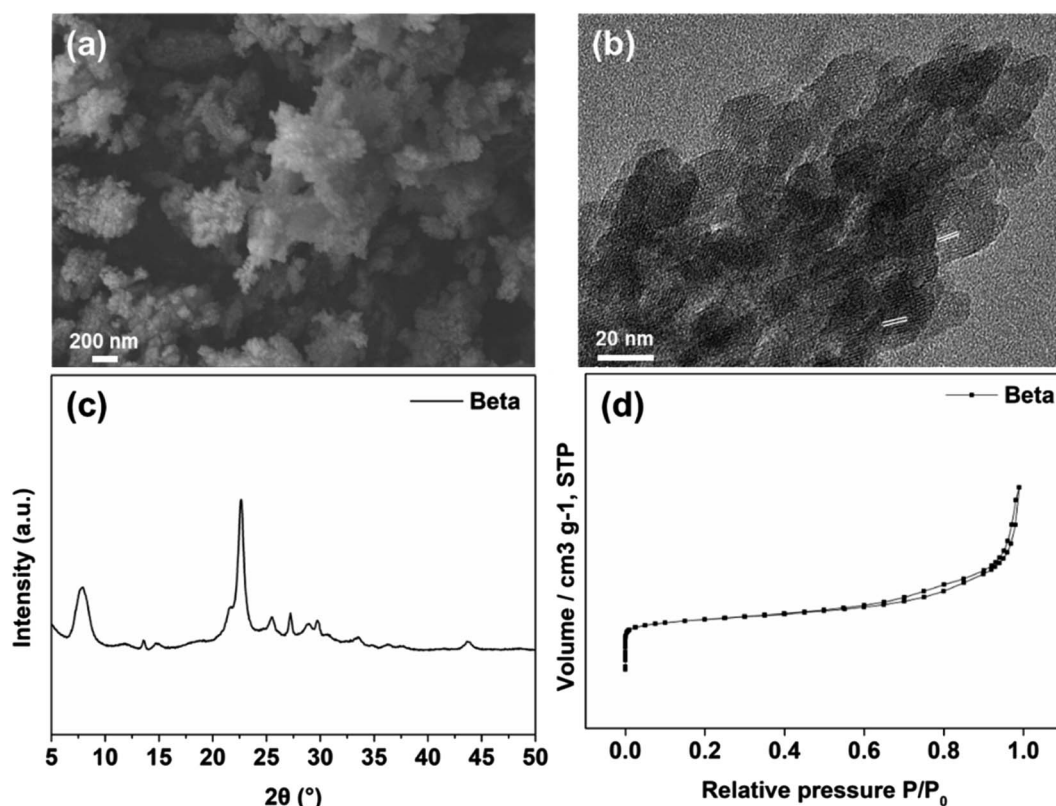


Fig. 2  (a) SEM image, (b) TEM image, (c) XRD patterns and (d) $N_2$ sorption isotherms of beta zeolite.
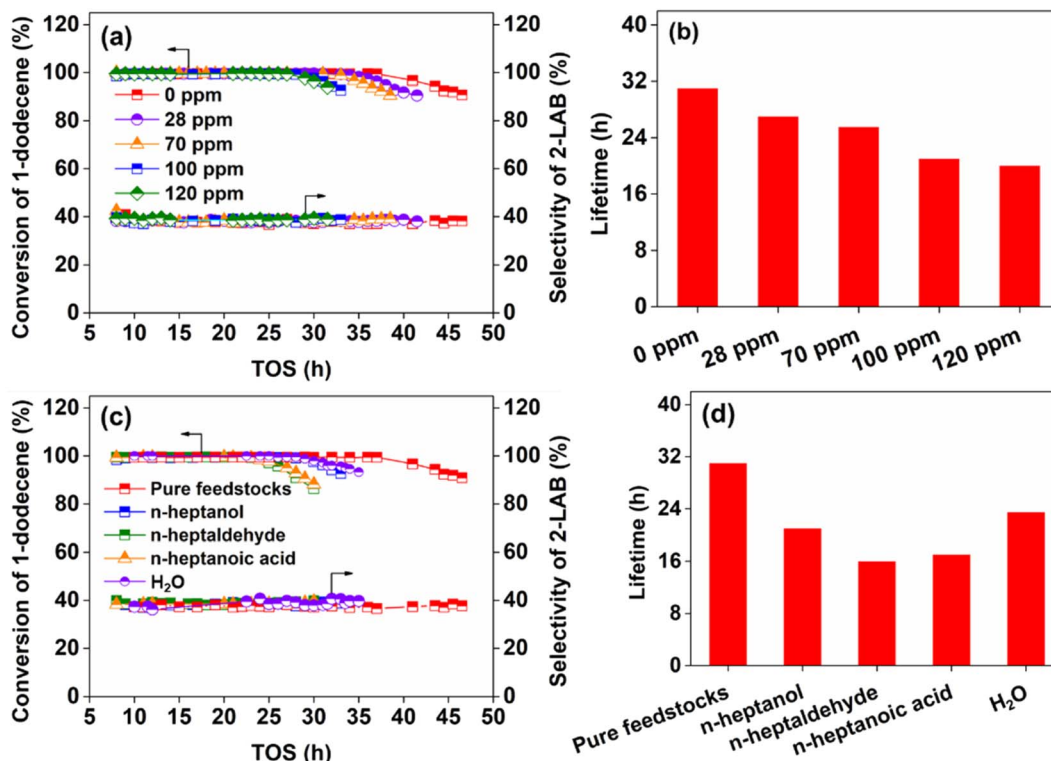
**Fig. 3** Effect of different oxygenated organic compounds on the alkylation of benzene with 1-dodecene. (a and b) Feedstocks contaminated with different amount of n-heptanol. (c and d) Comparison of different oxygenated organic compounds on the catalytic performance (100 ppm). Reaction conditions: 100 °C, 4.2 MPa, 15/1, 4 h$^{-1}$. The concentration of oxygenated organic compounds mentioned above is wt ppm, and this definition is used throughout the paper. TOS at the X axis denotes time on stream.

heptaldehyde and *n*-heptanoic acid) in the feedstocks,[45–48] we mainly discuss the effect of them in the present work. Additional discussion about the effect of H$_2$O can be found in Fig. S2 and S3.†

### 3.2. Deactivation mechanism and regeneration

In this part, we mainly discuss the deactivation at different conditions. As can be seen from Fig. 4a and Table 1, the surface areas of all the deactivated samples decrease sharply compared with the fresh one regardless of the pure or the oxygenated organic compounds contaminated feedstocks utilized. Generally, the decrease of zeolite surface areas was usually caused by the deposition of some organics on the inner and outer surfaces.[49–51] It's worth noting that the decrease of the surface area when feeding with pure feedstocks is larger than that of others, especially for the microporous surface areas. For beta zeolite, acid sites within the inner channels contribute a lot to the reactions. That's to say, most of the reactions occurred in
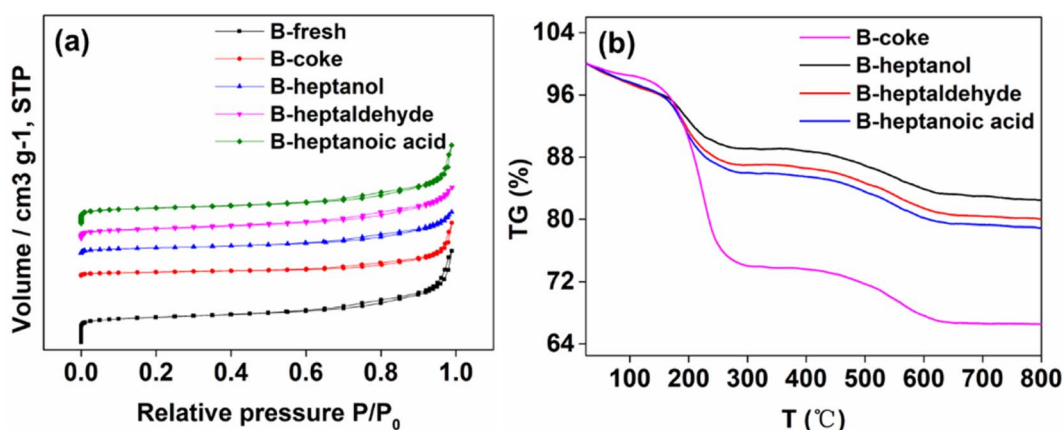


**Fig. 4** (a) N$_2$ sorption isotherms and (b) TG curves of different samples. The amounts of *n*-heptanol, *n*-heptaldehyde and *n*-heptanoic acid in the feedstocks were all 100 ppm.

Table 1  Texture properties of different samples

| Samples | Si/Al$^a$ | $S_{BET}{}^b$ (m$^2$ g$^{-1}$) | $S_{micro}{}^c$ (m$^2$ g$^{-1}$) | $S_{meso}{}^d$ (m$^2$ g$^{-1}$) | $V_{micro}{}^e$ (cm$^3$ g$^{-1}$) | $V_{meso}{}^f$ (cm$^3$ g$^{-1}$) | $V_{total}{}^g$ (cm$^3$ g$^{-1}$) |
|---|---|---|---|---|---|---|---|
| B-Fresh | 17.89 | 627 | 420 | 207 | 0.17 | 0.78 | 0.95 |
| B-Heptanol | — | 137 | 0 | 137 | 0.00 | 0.43 | 0.43 |
| B-Heptaldehyde | — | 231 | 24 | 207 | 0.01 | 0.52 | 0.53 |
| B-Heptanoic acid | — | 371 | 186 | 186 | 0.08 | 0.74 | 0.82 |
| B-Coke | — | 86 | 0 | 86 | 0.00 | 0.55 | 0.55 |
| M-Fresh$^h$ | 13.85 | 465 | 364 | 100 | 0.15 | 0.46 | 0.61 |

$^a$ The Si/Al ratio was measured by ICP-AES. $^b$ The total surface area was calculated by the BET method. $^c$ The micropore surface area was calculated using the $t$-plot method. $^d$ The mesopore surface area was calculated by the subtraction of $S_{BET}$ by $S_{micro}$. $^e$ The micropore volume calculated using the $t$-plot method. $^f$ The mesopore volume was calculated by the subtraction of $V_{total}$ by $V_{micro}$. $^g$ The total pore volume was obtained at a relative pressure of 0.98. $^h$ Ref. 32.

the inner channels.[21,33,52] However, the diffusion will become difficult at the same time when feeding reactants with large size, thus accelerating the reaction rate of side reactions. For the alkylation of benzene with 1-dodecene, 2-LAB is more desired, and the selectivity of it is highly correlated with the zeolite channels and 1-dodecene concentration. However, if the diffusion of reactants within the channels becomes difficult, the isomerization of 1-dodecene will be more likely to occur, thus decreasing the selectivity of 2-LAB. On the other hand, the lower selectivity of 2-LAB is always accompanied by the higher selectivity of other isomers. It's reported that the size of the dodecylbenzene isomers increases from 2-LAB to 6-LAB.[16,53] In such a way, the diffusion of molecules in the channels of beta will become more difficult with such large size products, which significantly increases the deactivation rate. In this way, the deactivation is usually caused by the blocking of large size molecule and coke, by which the surface areas decrease in a large extent. For the reactions feeding with oxygenated organic compounds contaminated feedstocks, the decreased surface areas are relatively less, implying a different deactivation mechanism.

The TG curves of different samples are shown in Fig. 4b. As can be seen, the weight loss of the deactivated sample when feeding pure feedstocks is much higher than that of the others, indicating that more molecules or molecules with larger size were adsorbed on it. This result is consistent with the texture properties discussed above. The IR spectra of different samples including the fresh and deactivated ones are shown in Fig. 5. As can be seen, two distinct peaks at ~2854 and ~2927 cm$^{-1}$ can be observed for all the deactivated samples additional to the fresh beta. According to the previous investigations, these two peaks are mainly attributed to –CH$_2$ and –CH$_3$ groups.[54,55] However, these two groups are included in all the feedstocks mentioned above, therefore it's difficult to get insight into the deactivated samples only by experimental techniques as discussed above. Therefore, we attempt to reveal the deactivation mechanism from theoretical point as follows.

Herein, DFT calculations were conducted to get insight into the effect of oxygenated organic compounds. It's reported that the orientations of the guest species in the zeolite channels have a great effect on their thermostability.[56–58] Accordingly, multi-geometry searching for the adsorption structures was firstly
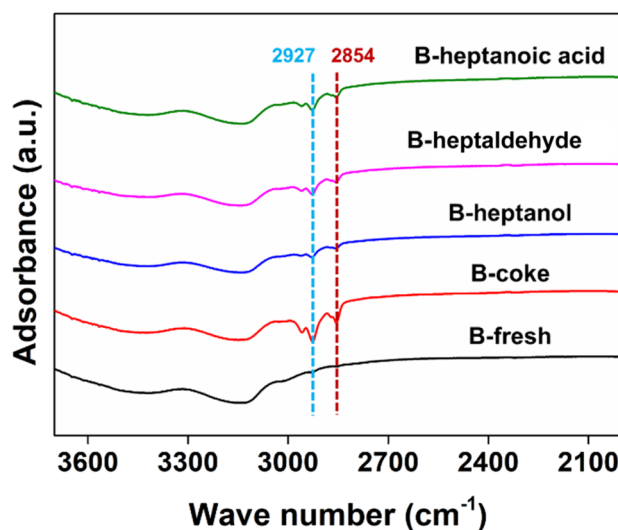


Fig. 5  IR spectra of different samples.

conducted (see Fig. S4†). The most stable configuration labelled $E_0$ is considered in the text (see Fig. 6). The adsorption energies of different molecules are shown in Fig. 6h. As can be seen, the adsorption energies of oxygenated organic compounds on the acid sites are larger than that of benzene, indicating the more competitive adsorption of them. However, the adsorption energy of 1-dodecene is much higher than that of others, including all the oxygenated organic compounds. This phenomenon was mainly due to its higher dispersion interaction with the channels of beta. Therefore, it not suitable to analyze the effect of oxygenated organic compounds only from the adsorption energy, especially for the reaction systems involving large size reactants. Further, the variation of the bond length of acid site O–H was also adopted as another descriptor to elucidate the proximity of different molecules to the acid sites. As shown in Fig. 6h, the variations of the O–H bond length aroused by the oxygenated organic compounds are much larger than that from both benzene and 1-dodecene, evidencing their higher proximity to the acid sites. Based on the discussion above, it can be concluded that the decreased lifetime when feeding with oxygenated organic compounds contaminated feedstocks should be mainly attributed to the higher proximity
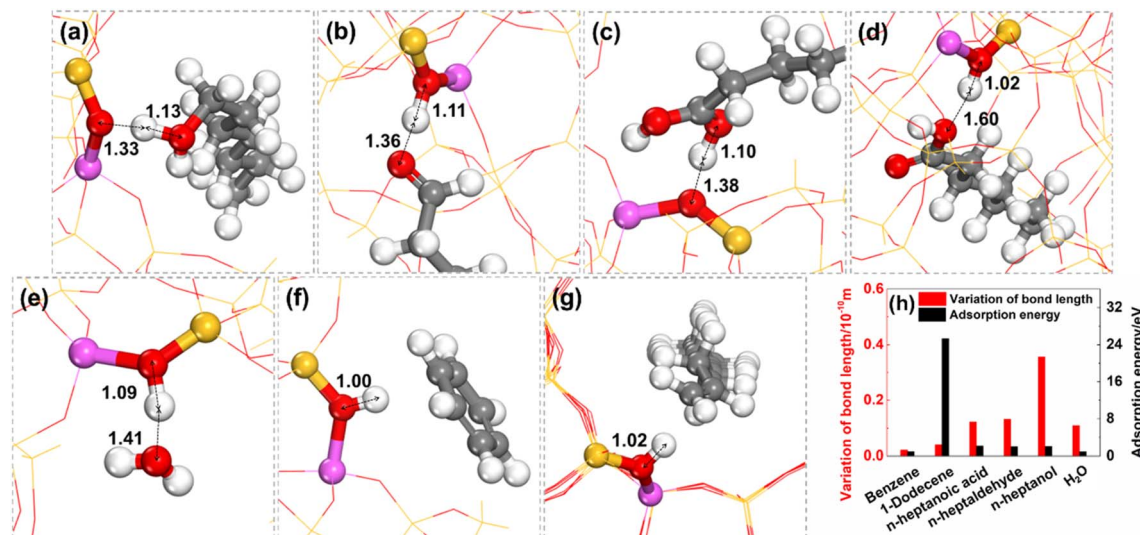
**Fig. 6** (a–g) Local geometry structures of the acid sites after adsorbing different molecules. (a) *n*-Heptanol, (b) *n*-heptaldehyde, (c) *n*-heptanoic acid (carbonyl), (d) *n*-heptanoic acid (hydroxyl), (e) H$_2$O, (f) benzene, (g) 1-dodecene. All distances are in Å. (h) Effect of different molecules on the variation of bond length of O−H and the corresponding adsorption energy.

of oxygenated organic compounds to the acid sites than that of benzene and 1-dodecene.

Generally, deactivation by coke usually occurs in the zeolite catalyzed reactions, especially for the reactions involving large-size reactants.[59–65] For the deactivated zeolite catalyst, extraction with organic solvents or coke-burning were usually adopted to regenerate the activity and lifetime.[60,65–67] For the reactions occurring in fixed-bed reactor, extraction with organic solvents is the primary choice,[60] and this method has been proved to be effective to recover the activity and lifetime completely.[68] Therefore, we firstly attempt to regenerate the deactivated catalysts by extraction with benzene at 250 °C. As can be seen from Fig. 7a and b, if the feedstocks were contaminated with trace amount of oxygenated organic compounds, the recovery rate of lifetime by extraction with hot benzene decreased gradually after 4 cycles, indicating that extraction with benzene can't

recover the lifetime effectively. Another method to regenerate the deactivated zeolite catalysts is coke-burning.[60,65–67] However, as can be seen from Fig. 7a and b, the lifetime decreased further after 5 h calcination at 500 °C in air flow, indicating the inefficiency of these methods when feeding with oxygenated organic compounds contaminated feedstocks. As discussed above, it can be concluded that it's significant to purify the long-chain α-olefins before used as feedstocks for the zeolite catalyzed LAB synthesis.

### 3.3. Comparison with MWW zeolite

In our previous investigation, MWW with open framework was selected to elucidate the effect of oxygenated organic compounds on the alkylation of benzene with 1-dodecene.[32] Combination with the discussion in the present work, it can be found that both of beta and MWW were all really sensitive to the
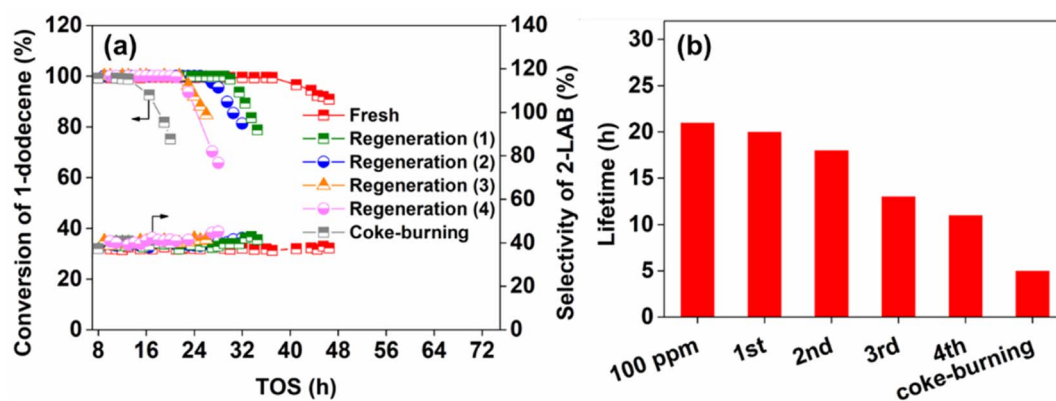


**Fig. 7** Regeneration by extraction with benzene and coke-burning. The feedstocks are mixed with 100 ppm *n*-heptanol. Reaction conditions: 100 °C, 4.2 MPa, 15/1, 4 h$^{-1}$. Regeneration conditions: 250 °C, 4.2 MPa, extraction with benzene, 4 h$^{-1}$, 24 h. Coke-burning was conducted at 500 °C for 4 h.
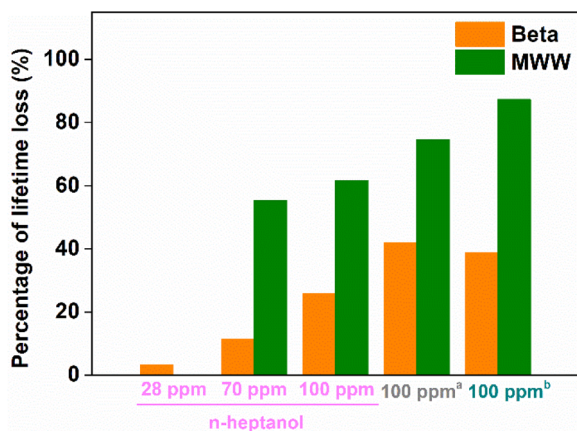
**Fig. 8** Comparison of the percentage of lifetime loss between beta and MWW.

oxygenated organic compounds added in the feedstocks, wherein trace amount of oxygenated organic compounds could cause obvious decrease of lifetime. On the other hand, the variations of surface areas of the deactivated catalysts were also consistent, although all the micropores were lost for beta when using pure feedstocks. Additionally, for the deactivated catalysts caused by oxygenated organic compounds, both of beta and MWW were all difficult to be regenerated whether by hot benzene extraction or coke-burning. And the deactivation of them were all mainly caused by the firm adsorption of oxygenated organic compounds on the acid sites.

However, there still exists some differences between them. As can be seen from Fig. 8. The percentages of lifetime loss of beta are distinctively less than that of MWW when adding the same amount of oxygenated organic compounds into the feedstocks. It's noteworthy that both of them suffered negligible lifetime loss when the amount of oxygenated organic compounds was below 28 ppm (beta: 3.2%; MWW: 0%). Obviously, beta is less sensitive to the oxygenated organic compounds contained in the α-olefins from Fischer–Tropsch synthesis than MWW.

As can be seen from Table 1, the surface area of beta is larger than that of MWW. For the alkylation of benzene with 1-dodecene, both micropores and mesopores of beta can all provide effective acid sites, wherein the reaction spaces are mainly provided by the micropores.[33] However, the effective acid sites over MWW are mainly located at the outer surface.[21] As can be seen from Table 2, the adsorption energies of all oxygenated organic compounds over beta are higher than that of MWW, and this is highly correlated with their structure differences. The acid sites of beta are mainly located at the inner channels,

wherein the molecules can be completely surrounded by the channel walls. However, MWW with the open framework can't provide sufficient dispersion interaction for the guest molecules, by which the adsorption energy over MWW is lower. According to the mechanism of the alkylation of benzene with olefins,[57,69,70] interaction of 1-dodecene with acid sites is the first step during the whole reaction process. Therefore, the catalytic performance was mainly determined by the competitive adsorption between 1-dodecene and oxygenated organic compounds. For the stronger interaction between 1-dodecene and the framework of beta, the adsorption energy of it is much higher than that of oxygenated organic compounds. That's to say, the oxygenated organic compounds can't replace 1-dodecene easily over beta. However, the results are different over MWW, wherein the adsorption energies of all oxygenated organic compounds are higher than that of 1-dodecene. Therefore, the activity of MWW was more sensitive to the oxygenated organic compounds.

On the other hand, there also exists some differences regarding the regeneration. As can be seen from Table 3, 64.52% of lifetime can be recovered for beta by extraction with benzene, while the lifetime of the regenerated MWW can only reach 31.92% of the fresh, indicating the oxygenated organic compounds adsorbed on beta can be washed off more easily than MWW. However, the results of coke-burning are different. As can be seen from Table 3, the recovery rate of MWW (68.42%) is much higher than that of beta (16.13%), implying that high temperature burning has less effect on the framework and acid sites of MWW. As can be seen from the XRD patterns shown in Fig. 9a and b, there are no obvious decrease of the crystallinity of beta and MWW after calcination, indicative of the high thermal stability of them. However, the loss percentage of acid amount is much higher for beta (see Fig. 9c and d, 40.43% for beta, 15.59% for MWW), which mainly accounts for its decreased lifetime.

As discussed above, these oxygenated organic compounds contained in the feedstocks are really detrimental to the zeolite catalyzed LAB synthesis. And it's also difficult to regenerate the deactivated catalysts by the general methods (e.g., extraction with hot benzene or coke-burning). Therefore, purification

**Table 3** Recovery rate (%) of beta and MWW by different regeneration methods (28 ppm n-heptanol)

| Samples | Extraction with benzene | Coke-burning |
|---------|-------------------------|--------------|
| Beta | 64.52 | 16.13 |
| MWW | 31.92 | 68.42 |

**Table 2** The adsorption energy of different molecules over beta and MWW (eV)

| Samples | Benzene | 1-Dodecene | n-Heptanol | n-Heptaldehyde | n-Heptanoic acid |
|---------|---------|------------|------------|----------------|------------------|
| Beta | 0.94 | 25.30 | 2.08 | 2.00 | 2.15 |
| MWW | 1.00 | 1.14 | 1.81 | 1.50 | 1.35 |

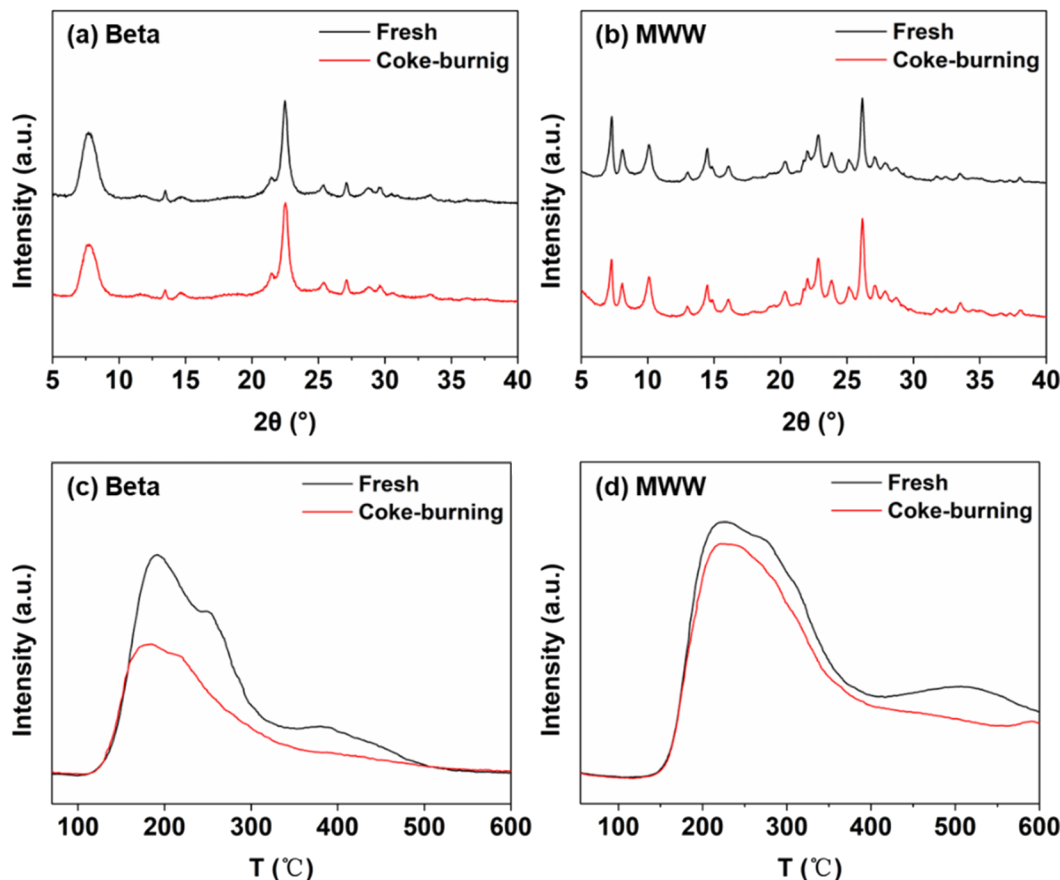© 2024 The Authors(s). Published by the Royal Society of Chemistry

**Fig. 9** XRD patterns and $NH_3$–TPD curves of (a and c) beta and (b and d) MWW before and after coke-burning.

seems necessary for the long-chain α-olefins from Fischer–Tropsch synthesis. Fortunately, an effective purification method has been proposed by our group, and the detailed operation procedures and results can be found in the ESI (see Fig. S5†).

## 4. Conclusion

In summary, the effect of oxygenated organic compounds (*n*-heptanol, *n*-heptaldehyde and *n*-heptanoic acid) on the catalytic performance of zeolite catalyzed LAB production, especially for the deactivation mechanism, has been studied. It's revealed that trace amount of oxygenated organic compounds could cause obvious decrease of lifetime. Firm adsorption of oxygenated organic compounds on the acid sites was proved to be the main reason for deactivation, and the deactivated catalysts were difficult to be regenerated by the general methods (extraction with hot benzene or coke-burning). Additionally, by comparing with the open-framework MWW zeolite, similar effect of oxygenated organic compounds on the catalytic performance and deactivation mechanism were obtained. However, beta is less sensitive to the oxygenated organic compounds, which is mainly due to the higher adsorption energy of 1-dodecene with its channels compared with that of MWW. Regeneration processes reveals that beta can be more easily regenerated by extraction with benzene compared with MWW. But contrary

results were observed for coke-burning, which is mainly due to more loss of acid sites of beta after calcination.

## Conflicts of interest

There are no conflicts to declare.

## Acknowledgements

## References

1 A. Aitani, J. B. Wang, I. Wang, *et al.*, Environmental Benign Catalysis for Linear Alkylbenzene Synthesis: A Review, *Catal. Surv. Asia*, 2014, **18**(1), 1–12.

2 G. D. Yadav and N. S. Doshi, Synthesis of Linear Phenyldodecanes by the Alkylation of Benzene with 1-Dodecene over Non-Zeolitic Catalysts, *Org. Process Res. Dev.*, 2002, **6**(3), 263–272.

3 L. Tian, J. Li, Y. Li, *et al.*, Synthesis of Dodecylbenzene with Benzene and 1-Dodecene over MCM-22 Zeolite Modified with Phosphorus, *Chin. J. Catal.*, 2008, **29**(9), 889–894.

4 J.-J. Wang, Y.-Y. Chuang, H.-Y. Hsu, et al., Toward industrial catalysis of zeolite for linear alkylbenzene synthesis: a mini review, Catal. Today, 2017, **298**, 109–116.

5 J. A. Kocal, B. V. Vora and T. Imai, Production of linear alkylbenzenes, Appl. Catal., A, 2001, **221**(1), 295–301.

6 F. Zarkesh, F. Farzaneh, M. Ghandi, et al., Metal ions exchanged montmorillonite as catalyst for alkylation of benzene with 1-dodecene, React. Kinet. Catal. Lett., 2006, **89**(2), 247–252.

7 S. R. Guerra, L. M. O. C. Merat, G. R. San, et al., Alkylation of benzene with olefins in the presence of zirconium-pillared clays, Catal. Today, 2008, **133**, 223–230.

8 T.-C. Tsai, I. Wang, S.-J. Li, et al., Development of a green LAB process: alkylation of benzene with 1-dodecene over mordenite, Green Chem., 2003, **5**(4), 404–409.

9 M. Han, C. Xu, J. Lin, et al., Alkylation of Benzene with Long-Chain Olefins Catalyzed by Fluorinated β Zeolite, Catal. Lett., 2003, **86**(1), 81–86.

10 A. R. A. S. Deshmukh, V. K. Gumaste and B. M. Bhawal, Alkylation of benzene with long chain (C8–C18) linear primary alcohols over zeolite-Y, Catal. Lett., 2000, **64**(2), 247–250.

11 J. A. Kocal, Detergent Alkylation Process Using a Fluorided Silica-Alumina, US Pat., US5196574A, 1991.

12 C. D. Chang, S. Han, J. G. Santiesteban, M. M. Wu and Y. Xiong, Process for Preparing Long Chain Alkylaromatic Compounds, US Pat., US5516954, 1994.

13 H.-O. Zhu, X.-Q. Ren and J. Wang, A comparative study of the catalytic behavior of SBA-15 supported heteropoly acid H3PW12O40 and H-Y catalysts in the alkylation of benzene with 1-dodecene, React. Kinet. Catal. Lett., 2004, **83**(1), 19–24.

14 W. Aslam, M. M. Hossain, M. A. Bari Siddiqui, et al., Kinetics of liquid phase alkylation of benzene with dodecene over mordenite, Can. J. Chem. Eng., 2015, **93**(5), 870–880.

15 P. B. Venuto, L. A. Hamilton, P. S. Landis, et al., Organic reactions catalyzed by crystalline aluminosilicates: I. Alkylation reactions, J. Catal., 1966, **5**(1), 81–98.

16 S. Sivasanker and A. Thangaraj, Distribution of isomers in the alkylation of benzene with long-chain olefins over solid acid catalysts, J. Catal., 1992, **138**(1), 386–390.

17 Y. Cao, R. Kessas, C. Naccache, et al., Alkylation of benzene with dodecene. The activity and selectivity of zeolite type catalysts as a function of the porous structure, Appl. Catal., A, 1999, **184**(2), 231–238.

18 W. Aslam, M. A. B. Siddiqui, J. B. Rabindran, et al., Selective synthesis of linear alkylbenzene by alkylation of benzene with 1-dodecene over desilicated zeolites, Catal. Today, 2014, **227**, 187–197.

19 J.-S. Lin, J.-J. Wang, J. Wang, et al., Catalysis of alkaline-modified mordenite for benzene alkylation of diolefin-containing dodecene for linear alkylbenzene synthesis, J. Catal., 2013, **300**, 81–90.

20 S. Xing, R. Zhang and M. Han, Structure/acid-reactivity relationship of the zeolite catalyzed alkylation of benzene with 1-dodecene by constructing micro-meso composites, Mol. Catal., 2022, **531**, 112703.

21 S.-Y. Xing, T.-F. Wang and M.-H. Han, Effect of different frameworks on the zeolite catalyzed alkylation of benzene with 1-dodecene, Mol. Catal., 2022, **531**, 112644.

22 G. C. Laredo, J. J. Castillo, J. Navarrete-Bolaños, et al., Benzene reduction in gasoline by alkylation with olefins: comparison of Beta and MCM-22 catalysts, Appl. Catal., A, 2012, **413–414**, 140–148.

23 P. G. Smirniotis and E. Ruckenstein, Alkylation of Benzene or Toluene with MeOH or C2H4 over ZSM-5 or beta. Zeolite: Effect of the Zeolite Pore Openings and of the Hydrocarbons Involved on the Mechanism of Alkylation, Ind. Eng. Chem. Res., 1995, **34**(5), 1517–1528.

24 G. Bellussi, G. Pazzuconi, C. Perego, et al., Liquid-Phase Alkylation of Benzene with Light Olefins Catalyzed by β-Zeolites, J. Catal., 1995, **157**(1), 227–234.

25 J. Fu and C. Ding, Study on alkylation of benzene with propylene over MCM-22 zeolite catalyst by in situ IR, Catal. Commun., 2005, **6**(12), 770–776.

26 R. Gounder and E. Iglesia, Catalytic Consequences of Spatial Constraints and Acid Site Location for Monomolecular Alkane Activation on Zeolites, J. Am. Chem. Soc., 2009, **131**, 1958–1971.

27 R. Gounder and E. Iglesia, Effects of Partial Confinement on the Specificity of Monomolecular Alkane Reactions for Acid Sites in Side Pockets of Mordenite, Angew. Chem., Int. Ed., 2010, **49**(4), 808–811.

28 K. Föttinger, G. Kinger and H. Vinek, 1-Pentene isomerization over FER and BEA, Appl. Catal., A, 2003, **249**(2), 205–212.

29 I. Amghizar, L. A. Vandewalle, K. M. Van Geem, et al., New Trends in Olefin Production, Engineering, 2017, **3**(2), 171–178.

30 H. H. Schobert and C. Song, Chemicals and materials from coal in the 21st century, Fuel, 2002, **81**(1), 15–32.

31 P. Tian, Y. Wei, M. Ye, et al., Methanol to Olefins (MTO): From Fundamentals to Commercialization, ACS Catal., 2015, **5**(3), 1922–1938.

32 S. Xing, Y. Cui, T. Wang, et al., Elucidating the effect of oxides on the zeolite catalyzed alkylation of benzene with 1-dodecene, Chin. J. Chem. Eng., 2023, **56**, 126–135.

33 R. Li, S. Xing, S. Zhang, et al., Effect of surface silicon modification of H-beta zeolites for alkylation of benzene with 1-dodecene, RSC Adv., 2020, **10**(17), 10006–10016.

34 G. Kresse and J. Furthmüller, Efficiency of ab-initio total energy calculations for metals and semiconductors using a plane-wave basis set, Comput. Mater. Sci., 1996, **6**(1), 15–50.

35 G. Kresse and J. Hafner, Ab initio molecular-dynamics simulation of the liquid-metal–amorphous-semiconductor transition in germanium, Phys. Rev. B: Condens. Matter Mater. Phys., 1994, **49**(20), 14251–14269.

36 S. Grimme, J. Antony, S. Ehrlich, et al., A Consistent and Accurate Ab Initio Parametrization of Density Functional Dispersion Correction (DFT-D) for the 94 Elements H-Pu, J. Chem. Phys., 2010, **132**, 154104.

37 P. E. Blöchl, Projector augmented-wave method, Phys. Rev. B: Condens. Matter Mater. Phys., 1994, **50**(24), 17953–17979.

38  G. Kresse and D. Joubert, From ultrasoft pseudopotentials to the projector augmented-wave method, *Phys. Rev. B: Condens. Matter Mater. Phys.*, 1999, **59**(3), 1758–1775.

39  H. J. Monkhorst and J. D. Pack, Special points for Brillouin-zone integrations, *Phys. Rev. B: Solid State*, 1976, **13**(12), 5188–5192.

40  *Structure Commision of the International Zeolite Association [R/OL]*, http://www.iza-structure.org/databases/.

41  Y.-L. Wang, X.-X. Wang, Y.-A. Zhu, *et al.*, Shape selectivity in acidic zeolite catalyzed 2-pentene skeletal isomerization from first principles, *Catal. Today*, 2020, **347**, 115–123.

42  M. Boronat, A. Corma, M. Renz, *et al.*, A Multisite Molecular Mechanism for Baeyer-Villiger Oxidations on Solid Catalysts Using Environmentally Friendly H2O2 as Oxidant, *Chemistry*, 2005, **11**, 6905–6915.

43  H. Fujita, T. Kanougi and T. Atoguchi, Distribution of Brønsted acid sites on beta zeolite H-BEA: a periodic density functional theory calculation, *Appl. Catal., A*, 2006, **313**(2), 160–166.

44  A. Andersen, N. Govind and L. Subramanian, Theoretical study of the mechanism behind the para-selective nitration of toluene in zeolite H-Beta, *Mol. Simul.*, 2008, **34**(10–15), 1025–1039.

45  J. K. Gorawara, H. Rastelli and J. Markovs, Process for Removal of Trace Polar Contaminants from Light Olefin Streams, *US Pat.*, US5271835[P/OL], 1993.

46  G. G. McGlamery Jr, J. H. Beech, *et al.*, Recycle of DME in an Oxygenate-To-Olefin Reaction System, *US Pat.*, US7989669[P/OL], 2011.

47  J. R. Lattner and D. R. Lumgair Jr, Method of Removing Oxygenate Contaminants from an Olefin Stream, *US Pat.*, US6838587[P/OL], 2005.

48  C. F. v. Egmond and D. J. Wilson, Method for Contaminants Removal in the Olefin Production Process, *US Pat.*, US8309776[P/OL], 2012.

49  W. Monama, E. Mohiuddin, B. Thangaraj, *et al.*, Oligomerization of lower olefins to fuel range hydrocarbons over texturally enhanced ZSM-5 catalyst, *Catal. Today*, 2020, **342**, 167–177.

50  X. Wang, X. Hu, C. Song, *et al.*, Oligomerization of Biomass-Derived Light Olefins to Liquid Fuel: Effect of Alkali Treatment on the HZSM-5 Catalyst, *Ind. Eng. Chem. Res.*, 2017, **56**(42), 12046–12055.

51  O. Jan, K. Song, A. Dichiara, *et al.*, Ethylene Oligomerization over Ni–Hβ Heterogeneous Catalysts, *Ind. Eng. Chem. Res.*, 2018, **57**(31), 10241–10250.

52  Y. Shi, E. Xing, W. Xie, *et al.*, Shape selectivity of beta and MCM-49 zeolites in liquid-phase alkylation of benzene with ethylene, *J. Mol. Catal. A: Chem.*, 2016, **418–419**, 86–94.

53  S. Sivasanker, A. Thangaraj, R. A. Abdulla, *et al.*, Shape Selective Alkylation of Benzene With Long Chain Alkenes Over Zeolites, *Studies in Surface Science and Catalysis*, ed. L. Guczi, F. Solymosi and P. Tétényi, Elsevier, 1993, pp. 397–408.

54  Z. Jin, L. Wang, E. Zuidema, *et al.*, Hydrophobic zeolite modification for in situ peroxide formation in methane oxidation to methanol, *Science*, 2020, **367**(6474), 193–197.

55  S. Cao, Y. Shang, Y. Liu, *et al.*, "Desert Rose" MCM-22 microsphere: synthesis, formation mechanism and alkylation performance, *Microporous Mesoporous Mater.*, 2021, **315**, 110910.

56  C.-M. Wang, Y.-D. Wang, Y.-J. Du, *et al.*, Computational insights into the reaction mechanism of methanol-to-olefins conversion in H-ZSM-5: nature of hydrocarbon pool, *Catal. Sci. Technol.*, 2016, **6**(9), 3279–3288.

57  D. Wang, C.-M. Wang, G. Yang, *et al.*, First-principles kinetic study on benzene alkylation with ethanol vs. ethylene in H-ZSM-5, *J. Catal.*, 2019, **374**, 1–11.

58  S. Xing, K. Liu, T. Wang, *et al.*, Elucidation of the mechanism and structure–reactivity relationship in zeolite catalyzed alkylation of benzene with propylene, *Catal. Sci. Technol.*, 2021, **11**(8), 2792–2804.

59  Z. Ma, X. Hou, B. Chen, *et al.*, Experiment and modeling of coke formation and catalyst deactivation in n-heptane catalytic cracking over HZSM-5 zeolites, *Chin. J. Chem. Eng.*, 2023, **55**(3), 165–172.

60  M. Díaz, E. Epelde, J. Valecillos, *et al.*, Coke deactivation and regeneration of HZSM-5 zeolite catalysts in the oligomerization of 1-butene, *Appl. Catal., B*, 2021, **291**, 120076.

61  X.-Y. Ren, J.-P. Cao, S.-X. Zhao, *et al.*, Insights into coke location of catalyst deactivation during in-situ catalytic reforming of lignite pyrolysis volatiles over cobalt-modified zeolites, *Appl. Catal., A*, 2021, **613**, 118018.

62  D. Rojo-Gama, M. Nielsen, D. S. Wragg, *et al.*, A Straightforward Descriptor for the Deactivation of Zeolite Catalyst H-ZSM-5, *ACS Catal.*, 2017, **7**(12), 8235–8246.

63  S. Inagaki, S. Shinoda, Y. Kaneko, *et al.*, Facile Fabrication of ZSM-5 Zeolite Catalyst with High Durability to Coke Formation during Catalytic Cracking of Paraffins, *ACS Catal.*, 2013, **3**(1), 74–78.

64  A. G. Gayubo, A. Alonso, B. Valle, *et al.*, Deactivation kinetics of a HZSM-5 zeolite catalyst treated with alkali for the transformation of bio-ethanol into hydrocarbons, *AIChE J.*, 2012, **58**(2), 526–537.

65  N. Chaouati, A. Soualah, M. Chater, *et al.*, Mechanisms of coke growth on mordenite zeolite, *J. Catal.*, 2016, **344**, 354–364.

66  Y. Nakasaka, T. Tago, H. Konno, *et al.*, Kinetic study for burning regeneration of coked MFI-type zeolite and numerical modeling for regeneration process in a fixed-bed reactor, *Chem. Eng. J.*, 2012, **207–208**, 368–376.

67  Y. Song, S. Liu, Q. Wang, *et al.*, Coke burning behavior of a catalyst of ZSM-5/ZSM-11 co-crystallized zeolite in the alkylation of benzene with FCC off-gas to ethylbenzene, *Fuel Process. Technol.*, 2006, **87**(4), 297–302.

68  X.-X. Li, Investigation on the Zeolite Catalyzed Alkylation of Benzene with Long-Chain α-olefins, MPhil thesis, Tsinghua University, 2018.

69  X. Rozanska, L. A. M. M. Barbosa and R. A. van Santen, A Periodic Density Functional Theory Study of Cumene Formation Catalyzed by H-Mordenite, *J. Phys. Chem. B*, 2005, **109**(6), 2203–2211.

70  Z. Lei, L. Liu and C. Dai, Insight into the reaction mechanism and charge transfer analysis for the alkylation of benzene with propylene over H-beta zeolite, *Mol. Catal.*, 2018, **454**, 1–11.